Impaired GABAergic transmission and altered hippocampal synaptic plasticity in collybistin-deficient mice

Theofilos Papadopoulos[1], Martin Korte[2], Volker Eulenburg[1], Hisahiko Kubota[1,3], Marina Retiounskaia[1], Robert J Harvey[4], Kirsten Harvey[4], Gregory A O'Sullivan[1], Bodo Laube[1], Swen Hülsmann[5], Jörg RP Geiger[3] and Heinrich Betz[1,*]

[1]Department of Neurochemistry, Max-Planck-Institute for Brain Research, Frankfurt, Germany, [2]Zoological Institute, Technical University Braunschweig, Braunschweig, Germany, [3]Independent Hertie Research Group, Max-Planck-Institute for Brain Research, Frankfurt, Germany, [4]Department of Pharmacology, The School of Pharmacy, London, UK and [5]Department of Neuro- and Sensory Physiology, University of Göttingen, Göttingen, Germany

Collybistin (Cb) is a brain-specific guanine nucleotide exchange factor that has been implicated in plasma membrane targeting of the postsynaptic scaffolding protein gephyrin found at glycinergic and GABAergic synapses. Here we show that Cb-deficient mice display a region-specific loss of postsynaptic gephyrin and $GABA_A$ receptor clusters in the hippocampus and the basolateral amygdala. Cb deficiency is accompanied by significant changes in hippocampal synaptic plasticity, due to reduced dendritic GABAergic inhibition. Long-term potentiation is enhanced, and long-term depression reduced, in Cb-deficient hippocampal slices. Consistent with the anatomical and electrophysiological findings, the animals show increased levels of anxiety and impaired spatial learning. Together, our data indicate that Cb is essential for gephyrin-dependent clustering of a specific set of $GABA_A$ receptors, but not required for glycine receptor postsynaptic localization.

Introduction

Fast synaptic transmission in the nervous system is mediated by ligand-gated ion channels, which are highly concentrated at postsynaptic membrane specializations. At inhibitory synapses, the scaffolding protein gephyrin is required for the synaptic localization of glycine receptors (GlyRs) and major $GABA_A$ receptor ($GABA_AR$) subtypes (Kneussel and Betz, 2000; Moss and Smart, 2001). Ablation of gephyrin expression by either antisense depletion in cultured neurons or gene knockout (KO) in mice prevents the clustering of GlyRs (Kirsch *et al*, 1993; Feng *et al*, 1998) and α2- and γ2-subunit containing $GABA_ARs$ (Essrich *et al*, 1998; Kneussel *et al*, 1999; Lüscher and Keller, 2004) at developing postsynaptic sites. The lack of postsynaptic inhibitory receptors is believed to underlie the early postnatal (day of birth, P0) lethality of gephyrin-deficient mice (Feng *et al*, 1998).

Gephyrin depends on both actin microfilaments and microtubules for synaptic targeting and submembraneous scaffold formation (Kirsch and Betz, 1995; Allison *et al*, 2000; Bausen *et al*, 2006; Maas *et al*, 2006) and binds to the cytoplasmic loop of the GlyR β-subunit (Meyer *et al*, 1995; Sola *et al*, 2004). In addition, the actin-binding proteins profilin (Mammoto *et al*, 1998) and Mena (mammalian enabled)/VASP (vasodilator stimulated phosphoprotein) (Giesemann *et al*, 2003; Bausen *et al*, 2006), as well as the dynein light chains 1 and 2 (Fuhrmann *et al*, 2002), interact with gephyrin.

Gephyrin also binds to collybistin (Cb) (Kins *et al*, 2000), a guanine nucleotide exchange factor (GEF) for small Rho-like GTPases. Multiple Cb splice variants (I–III) have been identified (Kins *et al*, 2000; Harvey *et al*, 2004a), and the human Cb homologue, hPEM-2, has been demonstrated to function as a GEF specific for Cdc42 in fibroblasts (Reid *et al*, 1999). Cb I and II share the catalytic DH and membrane-binding PH domains, but differ by the presence of an src homology 3 (SH3) region and a coiled-coil structure in Cb I. Coexpression of gephyrin with Cb II in human embryonic kidney (HEK) 293 cells alters the subcellular distribution of gephyrin by relocating it from large intracellular aggregates to small clusters at the cellular cortex (Kins *et al*, 2000). Cb has therefore been proposed to participate in a membrane activation process that labels postsynaptic membrane domains for inhibitory synapse formation (Kneussel and Betz, 2000). Indeed, overexpression of a Cb II deletion mutant lacking the PH domain interfered with clustering of gephyrin at synaptic sites (Harvey *et al*, 2004a). Furthermore, in a human patient suffering from hyperekplexia and epilepsy a mutation in the SH3 domain of Cb has been identified. Overexpression of this Cb mutant in cultured neurons resulted in the loss of postsynaptic gephyrin clusters (Harvey *et al*, 2004a). Together, these data point to an important role of Cb in gephyrin localization at inhibitory synapses.

To assess whether Cb is required for gephyrin-dependent clustering of inhibitory ionotropic receptors *in vivo*, we disrupted the Cb gene in mice. Herein, we show that in the absence of this neuronal GEF, gephyrin and gephyrin-dependent $GABA_AR$ subtypes, but not GlyRs, are lost from postsynaptic sites in specific brain regions. This results in reduced GABAergic transmission, altered hippocampal synaptic plasticity, increased anxiety scores and impaired spatial learning.

*Corresponding author. Department of Neurochemistry, Max-Planck-Institute for Brain Research, Deutschordenstrassee 46, 60528 Frankfurt am Main, Germany. Tel.: +49 69 96769 220; Fax: +49 69 96769 441; E-mail: neurochemie@mpih-frankfurt.mpg.de

Our study discloses an essential role of Cb at selected GABAergic synapses.

Results

Generation of Cb KO mice

To inactivate the mouse Cb gene (Arhgef9), located on the X-chromosome, in embryonic stem (ES) cells, we employed a targeting vector that allowed selective deletion of exon 5 by using the Cre-Lox system (Kuhn *et al*, 1995) (Figure 1A). Exon 5 encodes part of the catalytic RhoGEF domain, and its deletion is predicted to destroy exchange factor activity and to create a frameshift such that the entire C-terminus of Cb is lost. Using this strategy, we produced two independent properly targeted 'knockout' (KO) ES cell clones, which were injected into blastocysts to generate chimeric male mice. These animals were then crossed with C57BL/6 female mice to establish germline transmission of the mutation and to generate KO offspring. Mouse genotyping was carried out by Southern blot analysis of mouse tail DNA (Figure 1B). The absence of wild-type (WT) and truncated Cb transcripts and proteins in the Cb KO mice was confirmed by Northern blotting (Figure 1C) and Western blot analyses (Figure 1D), respectively.

Initial characterization of Cb KO mice

Female mice heterozygous for the Cb mutant allele (X^+X^-) appeared phenotypically normal and showed unimpaired

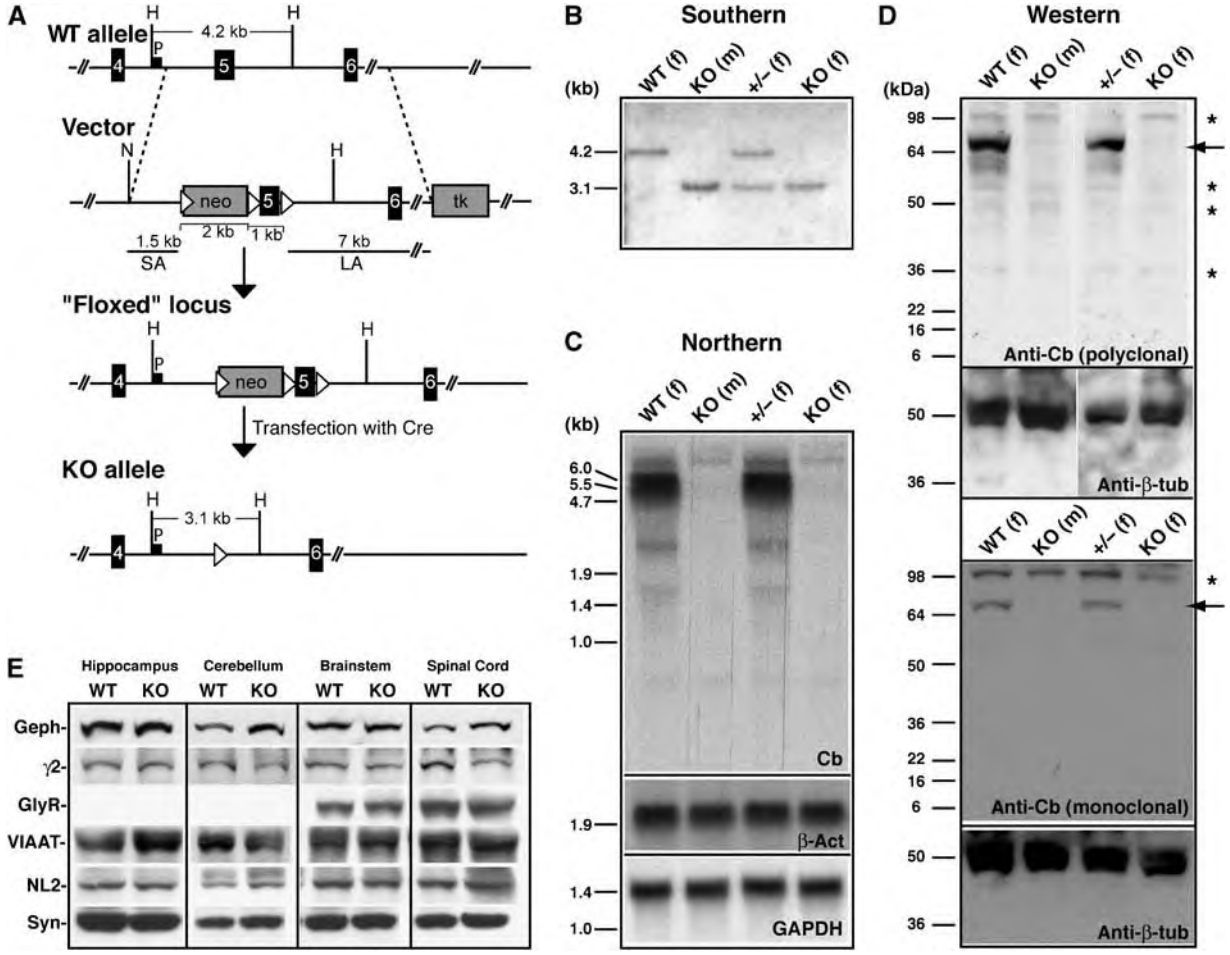

Figure 1 Targeted disruption of the mouse Cb gene. (**A**) Schematic representation of the targeting strategy showing the WT Cb gene, the targeting vector, the 'floxed' locus and the null allele. Exons are represented as black boxes. The neomycin resistance cassette (neo) and the herpes simplex virus thymidine kinase (tk) gene of the targeting vector are indicated as gray boxes, and loxP sites as triangles. P corresponds to the probe used for Southern analysis. SA, short arm; LA, long arm. Relevant restriction sites indicated are as follows: H, *Hin*dIII; N, *Not*I. (**B**) Southern blot analysis of *Hin*dIII-digested mouse tail DNA from WT, Cb KO and heterozygous (±) offspring. The 4.2 kb and the 3.1 kb bands represent the WT and the KO alleles, respectively. (m), male; (f), female. (**C**) Upper panel: Northern blot of brain total RNA with a 430-bp cDNA probe encoding exons 1–3 of the mouse Cb gene reveals 5.5 and 6.0 kb Cb transcripts in WT but not in Cb KO mice. Lower panels: control hybridizations with random-primed probes derived from a 714-bp fragment of the mouse β-actin (β-act) cDNA or a 490-bp fragment of the mouse GAPDH cDNA demonstrate that comparable amounts of total RNA were loaded. (**D**) Western blot analysis of brain homogenates (50 μg protein/lane) using either a polyclonal Cb antibody (upper panel) or a monoclonal antibody specific for the N-terminally located SH3 domain of the Cb protein (lower panel). Note the absence of Cb protein (indicated by arrows) in all KO samples. Asterisks indicate unspecific bands stained under the experimental conditions used. A β-tubulin (β-tub)-specific antibody was used to confirm that roughly equal amounts of protein were loaded. (**E**) Western blot analysis of crude membrane fractions prepared from different CNS regions of WT and Cb KO mice. Equal amounts of protein (50 μg protein/lane) were loaded and probed with the indicated antibodies. Note that the expression levels of all proteins tested were not significantly different between genotypes; densitometric scanning of the band intensities determined in three independent experiments did not reveal significant differences for any of the immunoreactive bands examined (data not shown). Geph, gephyrin; γ2, $GABA_AR$ γ2-subunit; GlyR, glycine receptor; VIAAT, vesicular inhibitory amino acid transporter; NL2, neuroligin 2; Syn, synaptophysin.

development and fertility. Crossing of the heterozygous female mice with C57BL/6 males, or intercrossing them with Cb KO (X^-Y) males, generated KO mice at Mendelian ratios. These animals also proved to be viable and fertile. For further analysis of the consequences of Cb deficiency, we focused on Cb KO males and their WT littermates. A histological analysis of cresyl-violet-stained sections from WT and KO brains failed to disclose differences in both brain size and morphology between genotypes (data not shown). Western blot analysis performed on hippocampal, cerebellar, brainstem and spinal cord membranes prepared from adult WT and Cb KO mice revealed that the immunoreactivities of the postsynaptic proteins gephyrin, the $GABA_AR$ γ2-subunit, the GlyR α-subunits and neuroligin 2, and of the presynaptic proteins VIAAT (vesicular inhibitory amino-acid transporter) and synaptophysin, all were similar in both genotypes (Figure 1E). Thus, inactivation of the Cb gene did not affect the expression of proteins found at inhibitory synapses.

Cb KO mice show normal locomotor behavior but enhanced anxiety

The motor performance of the Cb KO mice was normal at all postnatal stages examined. The mutant mice showed no signs of 'hind feet clasping', increased tremor or altered gait/righting responses, that is, symptoms indicative of impaired glycinergic inhibition (Gomeza *et al*, 2003). When locomotor behavior was tested in the open field, also no significant differences were detected between genotypes. Figure 2A and B indicate representative paths traveled by a WT (A) and a Cb KO (B) animal during an observation period of 10 min; the total path length covered by Cb KO mice was about 96% of that measured for the WT group (Figure 2C). Notably however, Cb KO mice spent significantly less time in the center than their WT littermates (Figure 2D), suggesting behavioral differences in anxiety-related responses between mutants and controls. Furthermore, in the elevated plus-maze, the KO mice spent significantly less time on the open arms than their WT littermates (Figure 2E). In addition, KO animals dipped their heads into the open arms less often than WT animals (Figure 2F). Thus, inactivation of the Cb gene resulted in a reduced exploratory behavior and increased anxiety scores without affecting motor performance.

Region-specific reduction of synaptic gephyrin and $GABA_AR$ clusters in the Cb KO CNS

As the expression levels of different synaptic proteins in the CNS of the Cb KO mice were unaltered (Figure 1E), we hypothesized that the observed behavioral deficits may be related to redistribution rather than loss of inhibitory postsynaptic proteins. Therefore, the postsynaptic localization of gephyrin was examined in brain sections prepared from adult WT and Cb KO mice. In WT sections, punctate gephyrin immunoreactivity was found throughout all CNS regions examined (Figure 3A, C and E). These gephyrin clusters were synaptically localized, as revealed by their apposition to presynaptic VIAAT immunoreactivity (Figure 3G, I and K). In contrast, brain sections derived from Cb KO mice showed region-specific reductions in the density of gephyrin clusters. The loss of punctate gephyrin immunoreactivity was most pronounced in hippocampal structures including the CA1–CA3 of stratum radiatum, stratum oriens (Figure 3B and J), dentate gyrus (hilus, molecular layer), lateral and ventral parts of the thalamus (data not shown), the amygdala (not shown) and the cerebellum (Purkinje cells, molecular layer; Figure 3D). In the granule cell layer of the olfactory bulb (not shown), the stratum pyramidale of the hippocampus (Figure 3B and H) and the granule cell and molecular layers of the cerebellum (Figure 3D), gephyrin was found in larger punctate structures that did not colocalize with VIAAT and corresponded to cytoplasmic gephyrin aggregates (data not shown). In contrast, when neocortex, striatum, medial thalamic areas, brainstem (caudal medulla) or spinal cord were analyzed, punctate gephyrin immunoreactivities were indistinguishable between KO and WT (Figure 3E, F, K and L, and data not shown). A summary of the anatomical results obtained is given in Supplementary Table I.

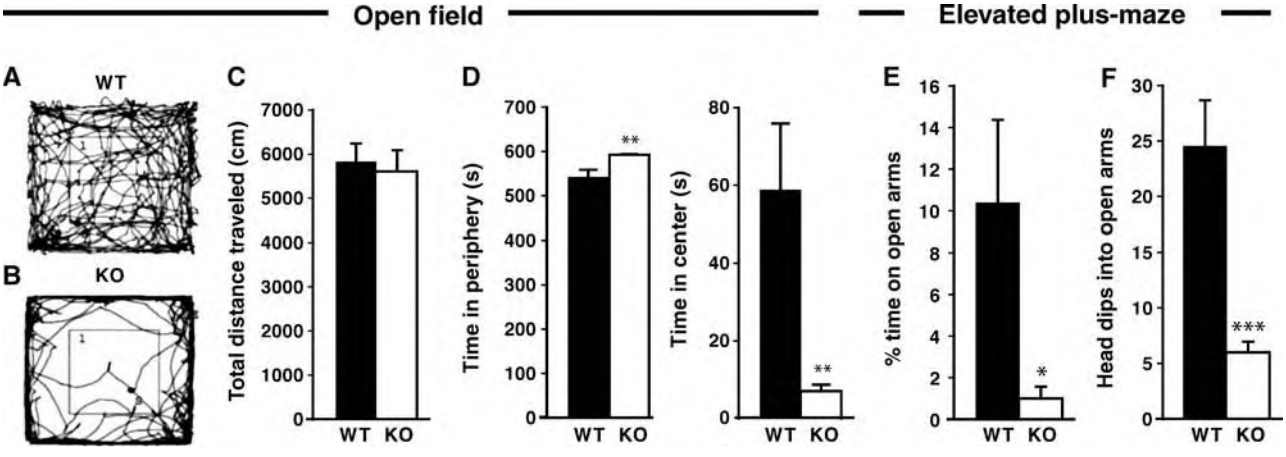

Figure 2 Behavior of Cb KO mice and WT littermates in the open field and elevated plus-maze tests. Male Cb KO mice and their WT littermates were tested between 8 and 10 weeks of age (open field, $n=10$ per group; elevated plus-maze, $n=7$ per group). All values represent means ± s.e.m. (**A–D**) Open field. (A, B) indicate representative paths traveled by a WT (A) and a Cb KO (B) animal during a period of 10 min. (C) No significant differences between genotypes were observed in the total distance traveled in the open field. (D) Cb KO mice showed a strong reduction in the time spent in the center of the open field and stayed significantly longer in the periphery as compared to WT (**$P<0.01$; Student's *t*-test). (**E, F**) Elevated plus-maze. (E) Cb KO mice spent less time on the open arms as compared with WT controls (*$P<0.05$; Student's *t*-test). (F) The number of head dips into open arms was strongly reduced with Cb KO animals as compared with WT littermates (***$P<0.001$; Student's *t*-test).

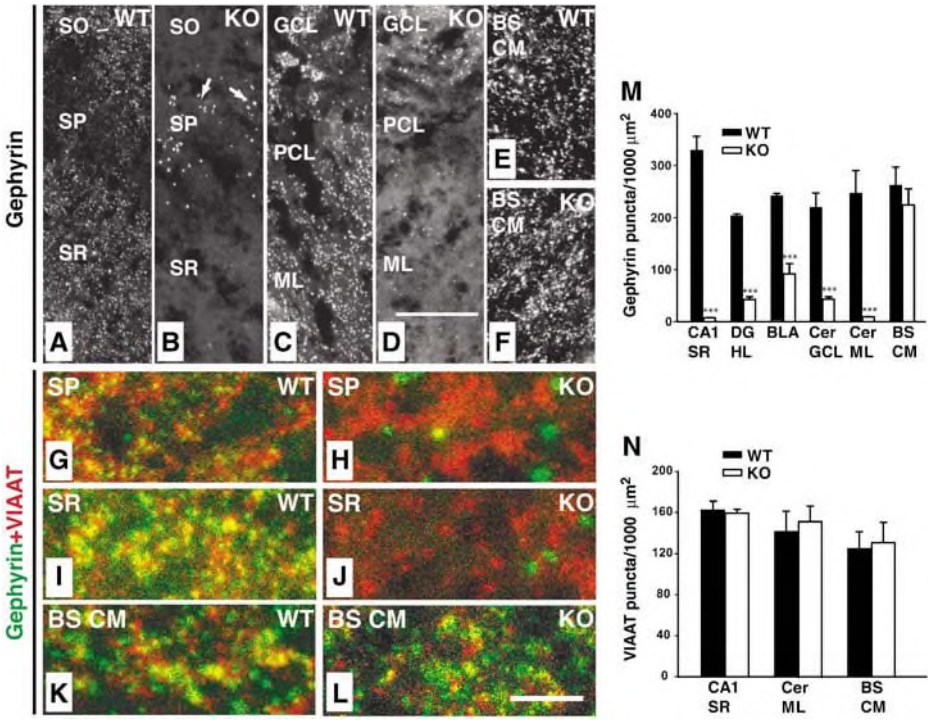

Figure 3 Region-specific reduction of synaptic gephyrin staining in the Cb KO CNS. (**A–L**) Sections from adult Cb KO mice and their WT littermates were stained with gephyrin and VIAAT antibodies. (A, B) The punctate staining of sections from KO animals for gephyrin was strongly reduced in the CA1 region of SR and SO as compared with WT sections. Note the significant increase of gephyrin deposits (arrows in B) in the SP of KO sections (A). (C, D) A strong reduction of gephyrin immunoreactivity was also observed in cerebellar regions (GCL, PCL, ML) of Cb KO animals. (E, F) BS CM sections in contrast showed similar densities of gephyrin puncta in both WT and KO animals. (G–L) Double immunostainings of gephyrin and VIAAT puncta in the SP (G, H) and SR (I, J) of the hippocampus, and in brainstem (K, L) of WT and Cb KO mice. Note that, in contrast to the loss of gephyrin puncta seen in (H, J), VIAAT immunoreactivity was unaffected by Cb deficiency (H, I). Scale bars, 32 μm (A–F), 16 μm (G–L). (**M, N**) Quantification of gephyrin and VIAAT immunoreactivities. For both genotypes, each bar corresponds to mean values (±s.e.m.) obtained with sections from 3–4 individual brains (***$P<0.001$; Student's *t*-test). SO, stratum oriens; SP, stratum pyramidale; SR, stratum radiatum; GCL, granule cell layer; PCL, Purkinje cell layer; Cer ML, molecular layer of cerebellum; BS CM, caudal medulla of the brainstem; DG HL, hilus of the dentate gyrus; BLA, basolateral amygdala.

Quantification of the number of gephyrin-immunoreactive puncta per 1000 μm^2 section area resulted in density values of 329±27 versus 7±0.6 for the stratum radiatum of the hippocampal CA1 region, 204±4 versus 43±5 for the hilus of the dentate gyrus, 240±5 versus 90±19.5 for the basolateral amygdala, 219±28 versus 43±5 for the granule cell layer of the cerebellum, 247±43 versus 9±0.5 for the molecular layer of the cerebellum, and 262±35 versus 225±31 for the brainstem (caudal medulla) in WT and Cb KO sections, respectively (Figure 3M). The number of VIAAT-immunoreactive sites was unaffected by the loss of Cb even in areas showing a marked reduction of gephyrin clusters (Figure 3N). This indicates that the density of inhibitory nerve terminals was not changed in the KO mice. Similar results were obtained when primary cultures of hippocampal neurons derived from WT and Cb KO littermate embryos were compared for dendritic gephyrin and VIAAT immunoreactivities (Supplementary Figure 1).

Since gephyrin is essential for synaptic clustering of both GlyRs (Feng *et al*, 1998; Harvey *et al*, 2004b) and α2- and γ2-subunit containing $GABA_A$Rs (Essrich *et al*, 1998; Kneussel *et al*, 1999, 2001a), we examined the effects of Cb deficiency on GlyR and $GABA_A$R localization. The distribution of GlyR clusters revealed by mAb4a staining was unchanged in three different CNS areas expressing GlyRs, the caudal medulla of the brainstem, the basolateral amygdala and the hilus of the dentate gyrus (Figure 4A–C). GlyR cluster numbers per 1000 μm^2 area were 327.8±22.7 versus 319.8±29.5 for brainstem, 29±2.8 versus 28.8±2.5 for the basolateral amygdala and 30.8±4.6 versus 35.5±3.5 for the hilus in WT and Cb KO sections, respectively (Figure 4D). Double labeling with mAb4a and the VIAAT antibody showed that only 28.8±3.4 and 27.9±2.7% of the GlyR clusters in the hilus of WT and Cb KO preparations, respectively, were apposed to VIAAT (data not shown). This low percentage of synaptic GlyR clusters in the hippocampus is in agreement with a previously published study (Danglot *et al*, 2004).

For examining the distribution of $GABA_A$Rs in the brain of Cb KO mice, we used an γ2-subunit-specific antibody. No significant difference was observed between WT and Cb KO sections in the number of $GABA_A$R γ2-immunoreactive puncta in brainstem (caudal medulla) and cerebellum (Figure 4E and H), as well as in spinal cord, neocortex, thalamus and striatum (Supplementary Table I, and data not shown). In contrast, we consistently found a strong reduction of $GABA_A$R γ2-subunit-positive puncta in the basolateral amygdala and the hippocampus of the Cb KO mice as compared with their WT littermates (Figure 4F, G and I; Supplementary Table I). Quantification of the number of γ2-positive clusters per 1000 μm^2 section area revealed density values of 188±13.5 versus 24±1 for the basolateral amygdala, 321±16.5 versus 51±2 for the hilus of the dentate gyrus,

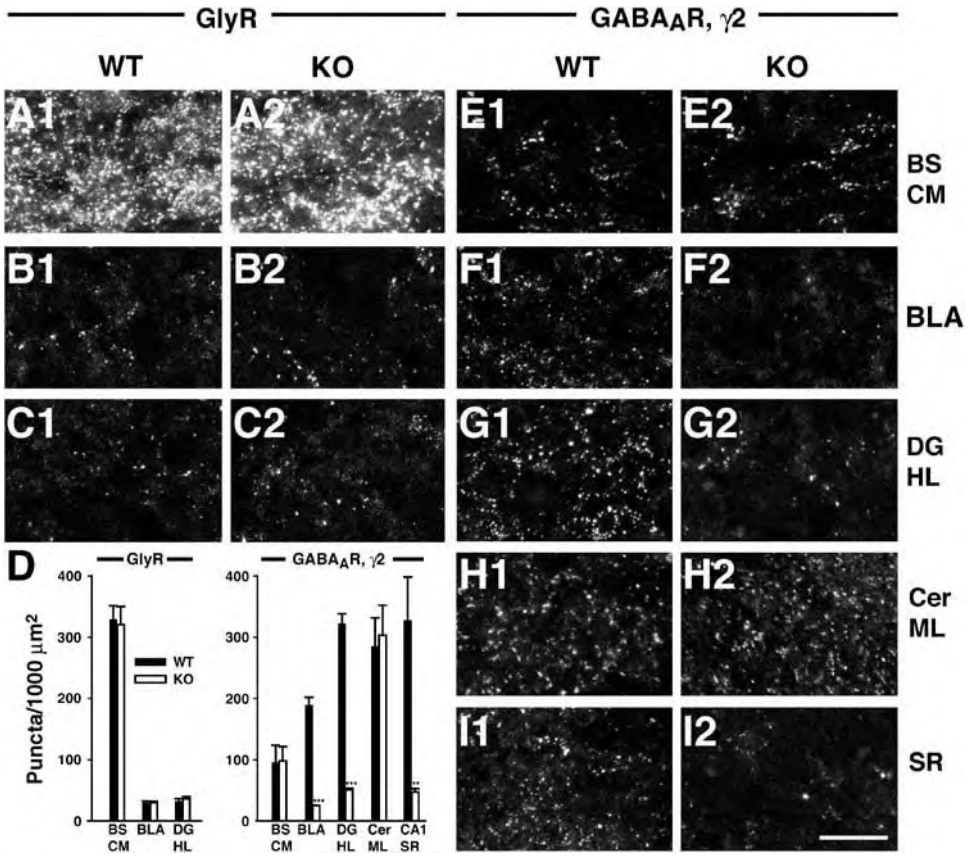

Figure 4 Reduced clustering of the $GABA_AR$ γ2-subunit in the hippocampus and basolateral amygdala of Cb KO mice. Sections from adult Cb KO mice and their WT littermates were stained with the GlyR specific mAb4a (**A–C**) or an antibody specific for the γ2-subunit of $GABA_ARs$ (**E–I**) and processed for confocal microscopy. (A–C) The punctate staining of GlyRs was comparable in BS CM, BLA and DG HL of both Cb KO and WT mice. (**D**) Quantification of GlyR and $GABA_AR$ γ2-subunit immunoreactivities. For both genotypes, each bar corresponds to counts performed on sections from 3–4 individual brains. Data represent means ± s.e.m. (**$P<0.01$; ***$P<0.001$; Student's *t*-test). (**E, H**) In BS CM and Cer ML, γ2-staining was unaffected by the loss of Cb, as compared to controls. (**F, G, I**) In contrast, the γ2-subunit punctate staining was selectively reduced in the BLA, the hilus of the DG and the CA1 region of SR in Cb KO sections, as compared with WT. Scale bar, 16 μm. BS CM, caudal medulla of the brainstem; BLA, basolateral amygdala; DG HL, hilus of the dentate gyrus; Cer ML, molecular layer of cerebellum; SR, stratum radiatum.

and 327 ± 71 versus 46.4 ± 5.3 for the stratum radiatum, in WT and Cb KO sections, respectively (Figure 4D). A similar reduction of gephyrin-dependent dendritic $GABA_AR$ clustering was observed when primary cultures of hippocampal neurons derived from WT and Cb KO littermate embryos were stained with a $GABA_AR$ α2-subunit-specific antibody (Supplementary Figure 1). In conclusion, Cb deficiency leads to a region-specific reduction of gephyrin-dependent $GABA_AR$ clusters.

Reduced dendritic GABAergic transmission in the hippocampus of Cb KO mice

To determine the physiological consequences of the reduced $GABA_AR$ γ2-subunit clustering seen in the hippocampus, we recorded GABAergic miniature inhibitory postsynaptic currents (mIPSCs) from CA1 pyramidal neurons in slices prepared from KO mice and littermate WT controls (Figure 5A and B). The most prominent difference found was a strong reduction (43.3%) in mean mIPSC frequency in KO neurons as compared with controls (WT: 3.3 ± 0.32 ms versus Cb KO: 1.87 ± 0.19 ms; $P<0.001$; Figure 5C). In addition, a significant decrease in the mean amplitude of mIPSCs (WT: 57.08 ± 2.74 pA versus Cb KO: 48.3 ± 2.53 pA; $P<0.05$; Figure 5B and D) and a slower rise time (WT: 1.31 ± 0.046 ms versus Cb KO: 1.57 ± 0.068 ms; $P<0.01$; Figure 5B and E) of mIPSCs was found in Cb KO mice, whereas mean mIPSC decay times were similar in both genotypes (WT: 24.59 ± 1.45 ms versus Cb KO: 22.67 ± 1.68 ms; $P=0.39$; Figure 5F). These results indicate postsynaptic changes and show that the loss of Cb results in a substantial reduction of action potential-independent GABAergic inhibition of CA1 pyramidal cells.

To test for action potential-dependent GABAergic inhibition, we performed experiments in brain slices and recorded evoked alpha-amino-3-hydroxy-5-methyl-4-isoxazole propionic acid (AMPA) receptor-mediated excitatory postsynaptic currents (EPSCs) and $GABA_AR$-mediated IPSCs from the somata of CA1 pyramidal cells (Supplementary data). However, the ratio of the peak amplitudes of GABAergic IPSCs and glutamatergic EPSCs was not significantly different between WT and Cb KO mice ($P>0.2$; data not shown). This might be explained by the fact that strong perisomatic inhibition (Freund, 2003), largely mediated by gephyrin-independent α1 containing $GABA_ARs$ (Kneussel *et al*, 2001a), masks differences in dendritic inhibition suggested by our immunohistochemical results (Figure 4; Supplementary

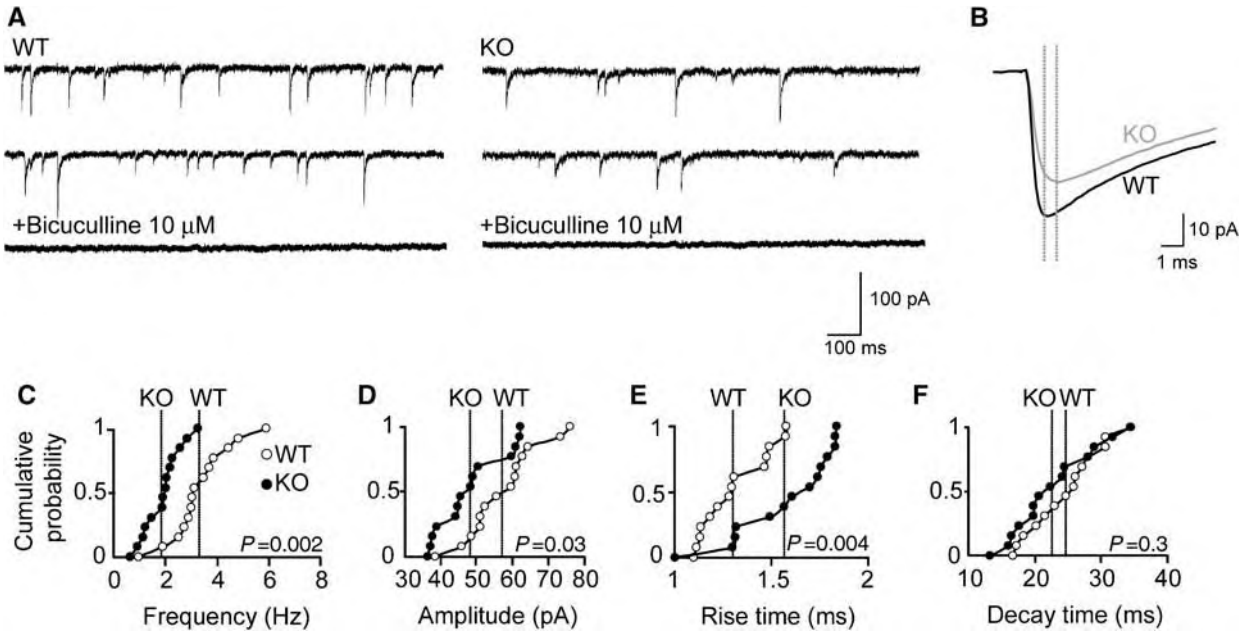

Figure 5 Altered GABAergic mIPSCs in CA1 pyramidal neurons of Cb KO slice preparations. (**A**) Representative traces of mIPSCs recorded in the absence or presence of the $GABA_A$ receptor antagonist bicuculline (10 μM) from WT and Cb KO neurons. (**B**) Superimposed averaged traces calculated from 3316 (WT) and 1316 (Cb KO) events over a recording period of 15 min. Dotted lines indicate peak positions of mIPSCs in each trace. (**C**–**F**) Cumulative distributions of mIPSC frequencies (C), amplitudes (D), rise times (E) and decay times (F) recorded from 14 neurons per genotype. In total, 40 351 (WT) and 23 370 (KO) events were analyzed. Each dot represents the mean value for an individual cell. Lines in each cumulative distribution indicate the averaged mean values of WT (open dots) and Cb KO (closed dots). *P*-values for each cumulative distribution are indicated (two-tailed Mann–Whitney *U*-test). All experiments were performed in the presence of 1 μM TTX, 10 μM CNQX and 1 μM D-AP5 at a V_H of −65 mV.

Figure 1). To disclose selective alterations in evoked dendritic inhibition, we performed field potential recordings on acute hippocampal slices by stimulating the Schaffer collateral-CA1 synapse and compared the local dendritic field potential response to extracellular stimulation both in the absence and presence of the $GABA_A$R antagonist picrotoxin (100 μM). Application of picrotoxin enhanced the slope of field excitatory postsynaptic potentials (fEPSPs) to a lesser extent in slices derived from Cb KO mice as compared with controls (WT: 130.1±4.1% versus Cb KO: 115.3±7.5%; $P=0.04$; Figure 6A), indicating a significant difference in GABAergic inhibition between genotypes. In conclusion, our analysis of mIPSCs and dendritic fEPSPs revealed a reduction of dendritic $GABA_A$R-mediated transmission in Cb KO mice.

Consistent with the unaltered punctate GlyR staining seen in brainstem of Cb KO mice, we found no differences in glycinergic neurotransmission between WT and KO animals. Recordings from hypoglossal motoneurons (Gomeza *et al*, 2003) disclosed similar mean amplitude (WT: 46.0±11.5 pA versus Cb KO: 54.0±6.5 pA; $P>0.1$), mean decay time (WT: 11.9±1.0 ms versus Cb KO: 11.9±0.6 ms; $P>0.1$) and mean frequency (WT: 9.7±3.5 Hz versus Cb KO: 7.8±2.6 Hz; $P>0.1$) values for glycinergic IPSCs in both genotypes.

Excitatory postsynaptic receptor function is unaffected in Cb KO mice

To assess whether the loss of Cb might affect excitatory synaptic transmission, we performed fEPSP recordings on slices derived from WT and Cb KO. This failed to reveal significant differences in basal parameters of excitatory synaptic transmission. In particular, the size of the presynaptic fiber volley (FV), which represents a good estimate of the number of stimulated axons, and the slope of fEPSPs were not significantly changed in mutant mice, although a trend to higher fEPSP slope values was noted in Cb KO mice (Figure 6B), consistent with reduced dendritic inhibition (Figure 6A). Furthermore, short-term plasticity, e.g. paired-pulse facilitation which is predominantly mediated by presynaptic mechanisms, was also unaltered (Figure 6C). To specifically analyze the functionality of the excitatory *N*-methyl-D-aspartate (NMDA) and AMPA receptors, fEPSPs were recorded under low (0.5 mM) Mg^{2+} conditions. In the presence of the NMDA receptor antagonist DL-2-amino-5-phosphonovalerate (AP-5) in the artificial cerebrospinal fluid (aCSF, low Mg^{2+}), the fEPSP slope was reduced to 71.3±7.4 and 73.6±5.1% in WT and Cb KO slices, respectively (Figure 6D). The remaining signal was completely AMPA receptor-dependent and disappeared in the presence of the selective AMPA receptor antagonist 6,7-dinitroquinoxaline 2,3-dione (DNQX) in both genotypes. This result suggests that NMDA and AMPA receptor transmission was unaffected in Cb KO mice. Consistent with these functional data, we also did not see any differences in the punctate staining of the excitatory synapse marker PSD-95 between WT and Cb KO hippocampal sections (data not shown).

Cb deficiency leads to changes in hippocampal synaptic plasticity

The reduction of dendritic GABAergic inhibition onto CA1 pyramidal neurons of Cb KO mice prompted us to investigate whether the induction of synaptic plasticity was affected in these animals. We analyzed the Schaffer CA3–CA1 hippocampal collateral pathway for deficits in two forms of activity-dependent synaptic plasticity, long-term potentiation

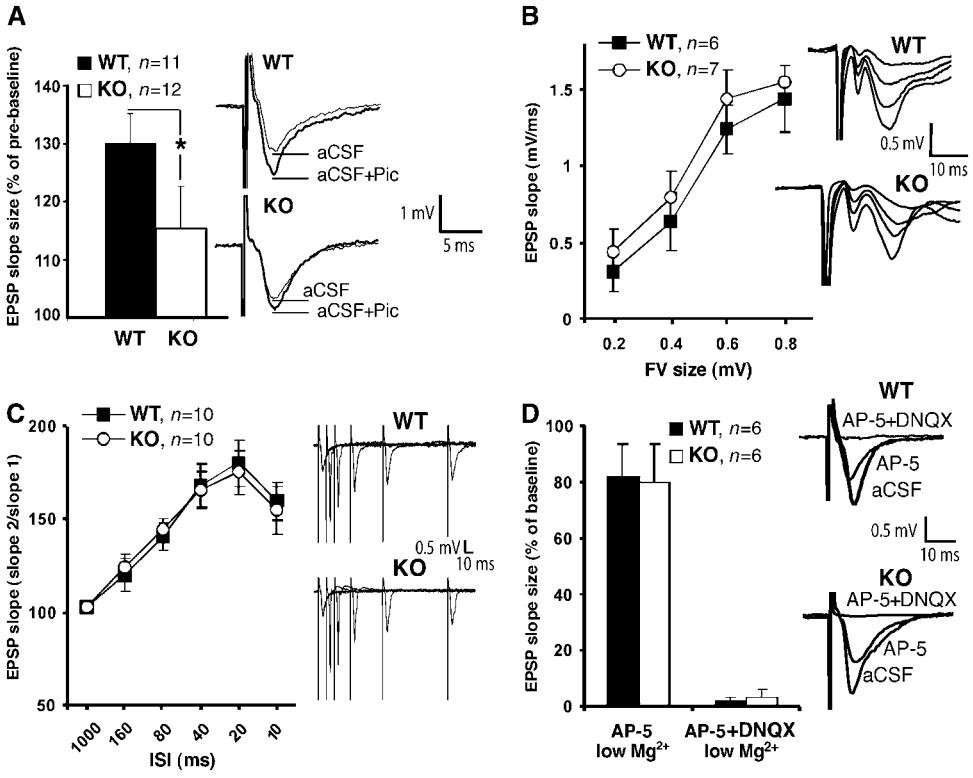

Figure 6 Analysis of fEPSPs in the hippocampal CA1 region. (**A**) Left: fEPSP slope size was significantly increased by bath-application of 100 μM picrotoxin. This enhancement was significantly larger in WT as compared with Cb KO mice (*$P<0.05$; two-tailed Student's *t*-test). Right: sweeps from individual experiments before (aCSF) and after application of picrotoxin (aCSF + Pic), averaged over three trials. (**B**) Left: fEPSP slope size at various stimulus intensities (FV: fiber volley). Right: series of original traces recorded from WT and Cb KO slices. (**C**) Left: paired-pulse facilitation of the fEPSP at various interstimulus intervals (ISI) from Cb KO and WT slices. Right: single sweeps for WT and Cb KO mice recorded at 10–160 ISI. (**D**) Left: NMDA receptor and AMPA receptor contributions to the fEPSP recorded in the presence of the indicated antagonists under low (0.5 mM) Mg^{2+} conditions. Right: original traces from individual experiments. In panels A–C, there were no significant differences between KO and WT slices ($P>0.1$; Student's *t*-test). All values represent means ± s.e.m.

(LTP) and long-term depression (LTD). LTP was induced by theta-burst stimulation (TBS) at 100 Hz. After recording a stable baseline, TBS was applied to fibers of the CA3 presynaptic neurons, and fEPSPs were recorded extracellularly in the stratum radiatum of the CA1 region for 3 h post stimulation. Short-term synaptic plasticity, measured as post-tetanic potentiation (PTP) after TBS, was unchanged in Cb KO mice (Figure 7A). However, comparison of KO mice with littermate WT controls revealed a significant increase in LTP, still visible 3 h after LTP induction (WT: 152.4 ± 9.7% versus Cb KO: 189.9 ± 14.5% at 175–180 min after TBS application; $P<0.001$; Figure 7A). As this might reflect an altered threshold of hippocampal LTP induction, we examined whether a 20 Hz tetanus was sufficient to induce LTP in Cb KO mice. Indeed, during the first 60 min after a 20 Hz TBS, significant potentiation was only seen in KO but not in control slices (WT: 101.4 ± 4.9% versus Cb KO: 118.8 ± 6.1%; $P<0.01$). However, fEPSP amplitudes were back to baseline 3 h after TBS application (data not shown).

To establish whether the altered threshold of hippocampal LTP induction seen in Cb KO animals is a consequence of reduced GABAergic neurotransmission, we induced maximal LTP by TBS (100 Hz) in the presence of the $GABA_AR$ antagonist picrotoxin (100 μM). Under these conditions, the difference in LTP noted between Cb KO slices and slices from WT littermates failed to be significant (WT: 168.9 ± 11.7% versus Cb KO: 185.3 ± 14.2% at 55–60 min after TBS application; $P=0.21$; Figure 7B). Moreover, comparison of the LTP induction produced in normal aCSF versus picrotoxin containing aCSF revealed an increase in potentiation only in slices derived from WT but not Cb KO mice (WT: $P=0.011$, Cb KO: $P=0.25$ for LTP induction in normal aCSF versus picrotoxin containing aCSF at 55–60 min after TBS application). Hence, the increased LTP seen in the mutant animals is due to reduced GABAergic inhibition.

In order to disclose whether synapses in Cb KO mice show a higher degree of plasticity, we analyzed depotentiation in Cb KO versus WT slices. We again induced maximal LTP by TBS (100 Hz), which after 5 min was followed by a low-frequency stimulus (LFS) (1 Hz) to induce depotentiation (Figure 7C). Using this protocol, it was not possible to depotentiate the fEPSPs recorded from Cb KO slices, whereas recordings from WT slices went back to baseline 60 min after LFS (WT: 104.7 ± 7.2% versus Cb KO: 166.3 ± 10.1%; $P<0.0001$).

Previous studies have demonstrated that depotentiation and homosynaptic LTD have many common properties (Bear and Abraham, 1996). We therefore examined whether LTD in the Schaffer collateral-CA1 pathway was also changed in the Cb KO slices. After recording baseline responses for 20 min, LFS was delivered to induce LTD. Whereas WT slices showed a persistent decrease in fEPSPs, which lasted for at least 1 h, the Cb KO slices returned to baseline (WT: 72.3 ± 4.6% versus Cb KO: 95.6 ± 5.4% at 55–60 min after LFS; $P<0.01$;

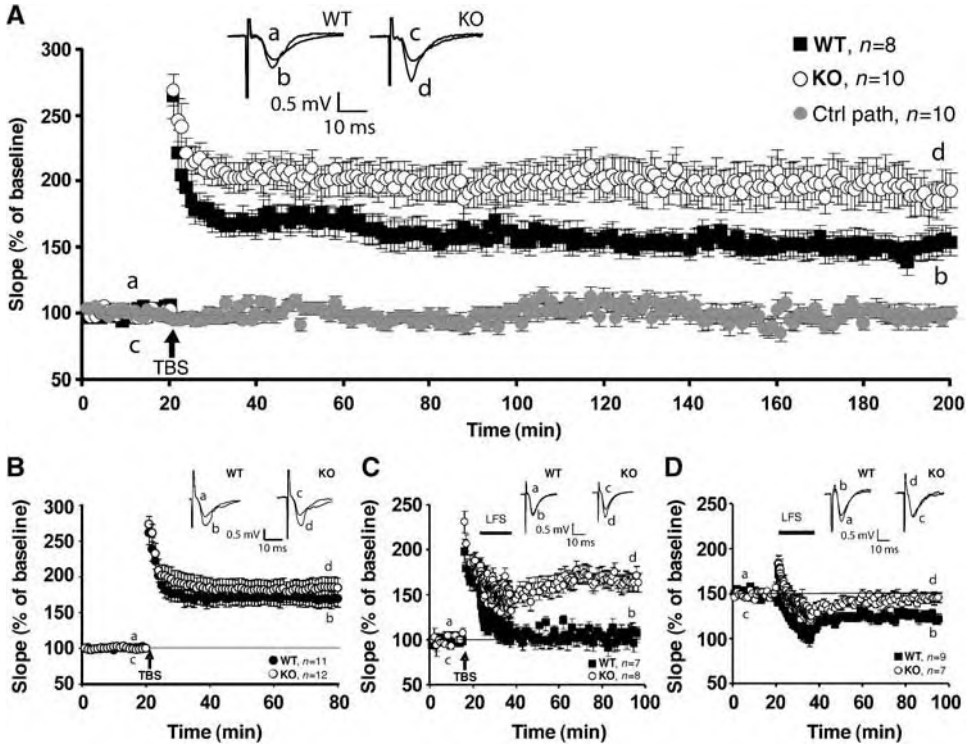

Figure 7 Cb KO mice show changes in synaptic plasticity. (**A**) LTP was induced in the CA3–CA1 pathway of the hippocampus in slices from WT ($n = 8$) and Cb KO ($n = 10$) mice; for all slices, a control pathway (ctrl path) was also recorded, here shown for the KO slices ($n = 10$). Inset shows sweeps from individual experiments at the time points indicated by a–d, averaged over six trials. The difference between genotypes was highly significant ($P < 0.001$; Student's *t*-test). (**B**) As (A), but in the presence of 100 μM picrotoxin ($n = 11$ for WT, $n = 12$ for Cb KO mice, respectively). Note that the difference between genotypes was no longer significant ($P = 0.38$; Student's *t*-test). (**C**) For depotentiation experiments, a TBS (100 Hz) was given, followed 5 min later by a 15 min LFS (1 Hz). WT slices ($n = 7$) displayed normal depotentiation (fEPSP amplitude goes back to baseline), whereas Cb KO slices ($n = 8$) showed no depotentiation effect ($P < 0.001$; Student's *t*-test). Inset shows sweeps from individual experiments as described in panel A. (**D**) In Cb KO slices, LTD was not induced upon LFS, whereas WT slices showed normal LTD ($P < 0.01$; Student's *t*-test). Inset shows sweeps from individual experiments as described in panel A.

Figure 7D). Thus, in Cb KO slices, the same LFS that was unable to reverse LTP when delivered 5 min after TBS, also failed to induce LTD. Overall, our results suggest a significant impairment of lasting bidirectional modifiability of CA1 pyramidal cell excitation (increased LTP and reduced LTD) in Cb KO mice.

Cb KO mice display deficits in spatial learning

The changes in synaptic plasticity observed in the hippocampus of Cb KO mice suggested that hippocampus-dependent memory formation might be affected in these animals. Therefore, we tested the Cb KO mice in a hippocampus-dependent learning paradigm, the spatial version of the Barnes maze (Barnes, 1979; Bach *et al*, 1995). In learning to find the escape tunnel, mice use a fixed sequence of three search strategies: random, serial and spatial (Supplementary data). Figure 8 presents the percentage of sessions, in which the animals used random (A), serial (B) or spatial (C) searches. Both WT and Cb KO mice employed the random search strategy in the first sessions (Figure 8A) and shifted to the more efficient serial search strategy subsequently (Figure 8B). However, although the KO mice were able to shift from random to serial search in a manner similar to that of WT animals, they used the spatial search strategy only at $<20\%$ of the time during the last sessions (days 25–30; Figure 8C). In contrast, the WT mice then spent $>80\%$ of the time with spatial searches. After day 17, 50% of the WT animals had learned to locate the escape tunnel, that is, acquired the task (Supplementary data), whereas none of the Cb KO mice did (Figure 8D). Even after 30 trials, 10 out of 10 Cb KO mice failed to show spatial memory, whereas 80% of the WT animals fulfilled the learning criterion (Figure 8D). A reversal test (Supplementary data) was performed with all mice that had learned successfully. Here, all animals displayed spatial retention during this trial (data not shown). In conclusion, the Cb KO mice developed normal hippocampal-independent serial searches (Bach *et al*, 1995), but appeared unable to learn the hippocampal-dependent spatial search strategy. These results suggest that the altered synaptic plasticity in the hippocampus of Cb KO mice is associated with an impairment in hippocampal-dependent memory formation.

Discussion

This study demonstrates that Cb is an essential determinant of gephyrin and $GABA_AR$ synaptic clustering in selected regions of the mammalian CNS. In Cb KO mice, the number of postsynaptically localized gephyrin and $GABA_AR$ γ2-subunit puncta was strongly reduced in the hippocampus and the basolateral amygdala. $GABA_ARs$ containing the α2- and γ2-subunits have been previously shown to depend on gephyrin for postsynaptic localization (Essrich *et al*, 1998; Kneussel *et al*, 1999). VIAAT immunocytochemistry failed to

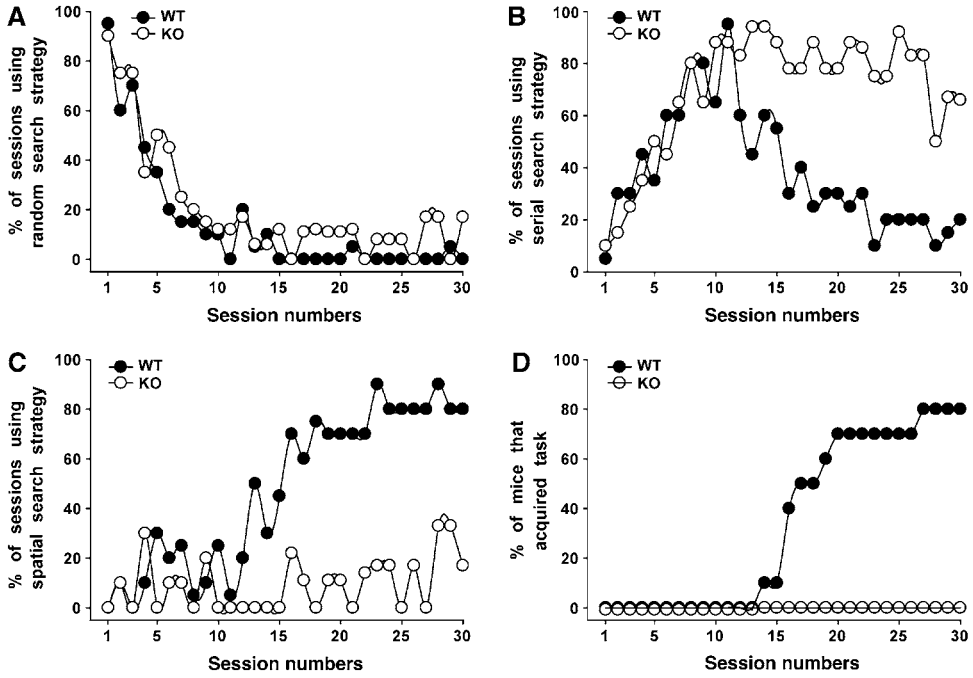

Figure 8 Barnes maze performance of WT and Cb KO mice. (**A–C**) The percentage of sessions, in which each of the three search strategies, (A) random, (B) serial and (C) spatial, was used by the WT and Cb KO mice, is presented. All sessions included the same number of animals per group ($n = 10$). (**D**) Plot showing the cumulative percentage of WT and Cb KO mice that had acquired the Barnes maze test over a period of 30 sessions.

reveal changes in the distribution and density of presynaptic terminals between KO and WT animals, indicating that the regional differences in gephyrin and $GABA_AR$ clustering do not reflect reduced inhibitory innervation. Notably, in neurons of some of the affected Cb KO brain regions, the loss of gephyrin clusters was accompanied by the appearance of cytoplasmic gephyrin immunoreactivity. This result is in agreement with previous data showing that coexpression of gephyrin with Cb II in HEK 293 cells alters the subcellular distribution of gephyrin by redistributing it from large intracellular aggregates to small clusters at the cellular cortex (Kins *et al*, 2000). Thus, our *in vivo* observations support the proposal that synaptically activated Cb binds to the cytoplasmic leaflet of the plasma membrane and thereby recruits gephyrin to developing postsynaptic sites (Kneussel and Betz, 2000). However, this seems to be true only for selected regions of the mammalian brain.

Our results extend the diversity of regulatory mechanisms underlying the formation, and possibly maintenance, of inhibitory postsynaptic membrane specializations by disclosing two types of gephyrin-dependent clustering reactions for inhibitory neurotransmitter receptors, Cb-dependent and Cb-independent ones. In contrast to what was predicted from previous transfection experiments (Kins *et al*, 2000; Harvey *et al*, 2004a), our results indicate that Cb is not essential for the gephyrin-dependent clustering of GlyRs in mice. On the other hand, gephyrin-mediated clustering of $GABA_ARs$ (Essrich *et al*, 1998; Kneussel *et al*, 1999) depends on Cb in a region-specific manner, as evidenced by the selective loss of major $GABA_AR$ subtypes from synapses in hippocampal and amygdala structures of the Cb KO mice. Furthermore, the unimpaired punctate staining of the $GABA_AR$ γ2-subunit in the cerebellum of the Cb KO mice, a region in which gephyrin clusters were strongly reduced, is in agreement with the existence of gephyrin-independent $GABA_AR$ clustering mechanisms as proposed previously (Kneussel *et al*, 2001a; Knuesel *et al*, 1999; Fischer *et al*, 2000; Sassoe-Pognetto *et al*, 2000; Levi *et al*, 2004).

The region- and receptor subtype-specific clustering impairment in Cb KO mice has important behavioral and functional consequences. In line with the unaffected GlyR clustering seen in the brainstem of Cb KO mice, we were unable to detect any neuromotor phenotype in these animals. However, in accordance with a region-specific loss of γ2-subunit containing $GABA_AR$ clusters, Cb KO mice showed an enhanced reaction to aversive stimuli, as demonstrated by two anxiety-related test paradigms, the open field and the elevated plus-maze. A similar anxiety phenotype has been observed in mice expressing only a single functional $GABA_AR$ γ2-subunit allele (Crestani *et al*, 1999). These anxiety-related responses are thought to be mediated by the septohippocampal and/or amygdala systems in both humans and animals, that is, the regions displaying reduced synaptic $GABA_AR$ staining in the Cb KO mice.

In the hippocampus of Cb KO mice, the marked reduction of dendritic $GABA_AR$ clusters correlated with a substantial decrease of GABAergic inhibition, as deduced from the analysis of mIPSCs recorded from CA1 pyramidal cells and pharmacological analysis of the dendritic fEPSPs. The most prominent effect was a significant reduction in mIPSC frequency, indicating a loss of functional synaptic sites. This could be interpreted as postsynaptic silencing of a large subset of inhibitory synapses due to the loss of clusters consisting largely of γ2-subunit containing $GABA_ARs$. In this scenario, postsynaptic $GABA_AR$ activation during GABA release from a single vesicle falls below electrophysiologically

detectable levels, resulting in a lower apparent mIPSC frequency. Additionally, the lack of postsynaptic $GABA_AR$ clusters could reduce presynaptic transmitter release probability, for example, by affecting retrograde signals. However, the number of GABAergic release sites appeared to be unchanged in the Cb KO mice, as inferred from VIAAT immunostaining. Electrophysiologically, a reduced GABAergic inhibition in the CA1 region of Cb KO mice could be directly demonstrated by pharmacological analysis of dendritic fEPSPs. However, we were unable to detect a general reduction of CA1 pyramidal cell inhibition when analyzing evoked IPSCs and EPSCs in the whole-cell configuration. This suggests that dendritic inhibition could not be resolved under these recording conditions, most likely due to the strong perisomatic innervation of the pyramidal cells by GABAergic interneurons. Notably, the synapses formed by parvalbumin-positive interneurons on CA1 pyramidal cells operate mostly via α1-subunit containing $GABA_ARs$ (Freund, 2003), which have been shown to not depend on gephyrin for postsynaptic localization (Kneussel *et al*, 2001a). Also, we cannot exclude a partial upregulation of perisomatically located $GABA_AR$ subunits other than γ2 in the hippocampus of the Cb KO mice.

Our analysis of synaptic plasticity in the hippocampal CA1 region shows that Cb deficiency causes significant changes in LTP, LTD and depotentiation. This cannot be attributed to changes in excitatory transmission, since our fEPSP analysis of fiber volley size, paired-pulse facilitation and glutamate receptor pharmacology were not significantly different between genotypes. Apparently, the reduction of dendritic GABAergic inhibition shifts the threshold for induction of lasting synaptic plasticity toward LTP under the experimental protocols used. Consistent with this interpretation, in the presence of the $GABA_AR$ antagonist picrotoxin, the difference in LTP induction seen between WT and Cb KO slice preparations was occluded. In agreement with our findings, a previous report has shown that hyperexcitability induced by GABA withdrawal decreases the threshold of LTP induction due to reduced $GABA_AR$-mediated inhibitory activity (Casasola *et al*, 2004).

Different studies indicate that bidirectional modifiability of synaptic strength is critical for a neuronal network to function as an effective memory system (Huh *et al*, 2000; Zeng *et al*, 2001). Consistent with this view, the impairment of spatial learning observed in Cb KO mice correlates with both enhanced LTP and reduced LTD in the hippocampal CA1 region of these mice. Although changes in other GABAergic circuits where gephyrin deposition also depends on Cb function could contribute to impaired spatial learning, we consider this highly unlikely. Clearly the Cb KO mice were not impaired in motivation, as deduced from their motility in the Barnes maze paradigm and the efficient acquisition of the serial search strategy. Furthermore, enhancement of hippocampal LTP in combination with spatial memory impairment has been previously seen in PSD-95- (Migaud *et al*, 1998), GluR2- (Gerlai *et al*, 1998) and dystrophin-(Vaillend *et al*, 2004) deficient mice. Together, these data suggest that under conditions, which cause many synapses within a network to become strongly potentiated (e.g., due to reduced GABAergic inhibition), degradation of information storage might occur, which becomes manifest as a learning impairment (Migaud *et al*, 1998). Taken together, our results indicate that Cb has an essential role in inhibitory synapse specification and thereby contributes to the balance of excitation and inhibition, which constitutes an important determinant of synaptic plasticity in the hippocampus.

Cb was originally identified as a brain-specific GEF, whose transcripts are widely distributed throughout the mammalian CNS (Kins *et al*, 2000; Kneussel *et al*, 2001b). Cb mRNA prominently accumulates during the second half of embryonic development and increases until the adult stage, consistent with a role of Cb in neuronal development and/or synaptogenesis. The reasons for the discrepancy between the widespread expression of Cb and the region-specific roles disclosed here are currently unknown but might reflect compensation or interaction specificity. During the last decade, many brain-specific GEFs have been identified, which have been implicated in different neuronal processes (Schmidt and Hall, 2002). Interestingly, some of these neuronal GEFs display high sequence similarity to Cb (Thiesen *et al*, 2000) and might therefore substitute for Cb in a developmental stage- or region-specific manner. Furthermore, gephyrin is known to exist in different splice variants, some of which have been reported to display tissue-specific expression (Prior *et al*, 1992; Ramming *et al*, 2000; Ule *et al*, 2003; Paarmann *et al*, 2006). Hence, the interaction of Cb with gephyrin (Grosskreutz *et al*, 2001) might be regulated by alternative splicing or secondary protein modification reactions. Clearly, further work is required to unravel the molecular mechanisms underlying the region- and synapse-specific regulation of postsynaptic gephyrin clustering.

Materials and methods

Generation of Cb KO mice

For the generation of Cb KO mice, a previously used strategy was employed (Harvey *et al*, 2004b). For details see Supplementary data.

RNA isolation and Northern blotting

Total RNA was isolated from WT and Cb KO brains by using TRIZOL reagent (Invitrogen, Karlsruhe, Germany). For details see Supplementary data.

Western blotting

Brain homogenates or crude membrane fractions from mouse hippocampus, cerebellum, brainstem or spinal cord were prepared as described (Kneussel *et al*, 1999), separated by 10 or 7.5% SDS–polyacrylamide gel electrophoresis (20–50 μg protein/lane), transferred to nitrocellulose (Schleicher & Schüll, Dassel, Germany), and probed with different primary antibodies as detailed in Supplementary data. Bound antibody was visualized using an enhanced chemiluminescence detection system (Perbio Science, Bonn, Germany).

Immunostaining

Cryostat sections (14 μm) were prepared, fixed and stained with mAb7a against gephyrin and a VIAAT antibody as described (Kirsch and Betz, 1995; Feng *et al*, 1998). Immunostainings were performed similarly for all brain regions analyzed. Immunostaining with an antibody against the $GABA_A$ receptor γ2-subunit or mAb4a, which recognizes all GlyR α-subunits, was performed as described in Supplementary data. Incubation with secondary antibodies was performed as described (Kirsch and Betz, 1995). Images were collected by confocal microscopy, as detailed in Supplementary data.

Electrophysiological recordings of GABAergic mIPSCs from acute hippocampal slices

For slice electrophysiology, 5- to 6-week-old mice were anaesthetized with isoflurane and decapitated according to institutional

guidelines. Transverse 300-μm thick hippocampal slices were cut using a custom-built vibratome (Geiger *et al*, 2002). Whole-cell patch-clamp recording of GABAergic mIPSCs from CA1 pyramidal neurons was performed as described in Supplementary data.

Electrophysiological recordings from acute hypoglossal slices

Two hundred and eighty micrometer slices of the caudal medulla containing the hypoglossal nucleus from P6-P8 mice were prepared, and spontaneous glycinergic IPSCs in WT ($n=11$) and Cb KO ($n=8$) neurons were recorded as described previously (Gomeza *et al*, 2003).

Field potential recordings on acute hippocampal slices

LTD experiments were performed with P14-P20 mice. Mice used for LTP and depotentiation experiments were P40–P70. Slice preparation, electrophysiological recordings, pharmacology and data analysis were performed as described previously (Rosch *et al*, 2005). For LTP experiments in the presence of picrotoxin (100 μM), a cut was introduced with a razor blade between the CA3 and CA1 region, in order to prevent seizure activity. The baseline recorded for 20 min before high-frequency stimulation was stable in the presence of picrotoxin, which was added to the aCSF 10 min before starting the baseline (10 min 'prebaseline' condition), and hence 30 min before TBS application. The effect of picrotoxin on fEPSP slope was analyzed by comparing fEPSPs recorded 5 min before picrotoxin application with those sampled in the presence of picrotoxin during the first 5 min of prebaseline recording. Then the relative contribution of evoked dendritic inhibition to the fEPSP slope size was compared between WT and Cb KO mice.

Behavioral studies

Behavioral tests were performed as detailed in Supplementary data.

Supplementary data

Supplementary data are available at *The EMBO Journal* Online (http://www.embojournal.org).

Acknowledgements

We thank Dr Klaus Rajewsky for the gift of pEasyFlox, Drs Joachim Kirsch, Nils Brose and Jean-Marc Fritschy for providing antibodies, and Ina Bartnik, Angela Traudt and Arne Buschler for slice preparation. This work was supported by the Max-Planck-Gesellschaft, Deutsche Forschungsgemeinschaft (SFB-628/P15), Fonds der Chemischen Industrie, Hertie Foundation and Medical Research Council (UK).

References

Allison DW, Chervin AS, Gelfand VI, Craig AM (2000) Postsynaptic scaffolds of excitatory and inhibitory synapses in hippocampal neurons: maintenance of core components independent of actin filaments and microtubules. *J Neurosci* **20:** 4545–4554

Bach ME, Hawkins RD, Osman M, Kandel ER, Mayford M (1995) Impairment of spatial but not contextual memory in CaMKII mutant mice with a selective loss of hippocampal LTP in the range of the theta frequency. *Cell* **81:** 905–915

Barnes CA (1979) Memory deficits associated with senescence: a neurophysiological and behavioral study in the rat. *J Comp Physiol Psychol* **93:** 74–104

Bausen M, Fuhrmann JC, Betz H, O'Sullivan GA (2006) The state of the actin cytoskeleton determines its association with gephyrin: Role of ena/VASP family members. *Mol Cell Neurosci* **31:** 376–386

Bear MF, Abraham WC (1996) Long-term depression in hippocampus. *Annu Rev Neurosci* **19:** 437–462

Casasola C, Montiel T, Calixto E, Brailowsky S (2004) Hyperexcitability induced by GABA withdrawal facilitates hippocampal long-term potentiation. *Neuroscience* **126:** 163–171

Crestani F, Lorez M, Baer K, Essrich C, Benke D, Laurent JP, Belzung C, Fritschy JM, Lüscher B, Mohler H (1999) Decreased $GABA_A$-receptor clustering results in enhanced anxiety and a bias for threat cues. *Nat Neurosci* **2:** 833–839

Danglot L, Rostaing P, Triller A, Bessis A (2004) Morphologically identified glycinergic synapses in the hippocampus. *Mol Cell Neurosci* **27:** 394–403

Essrich C, Lorez M, Benson JA, Fritschy JM, Lüscher B (1998) Postsynaptic clustering of major $GABA_A$ receptor subtypes requires the gamma 2 subunit and gephyrin. *Nat Neurosci* **1:** 563–571

Feng G, Tintrup H, Kirsch J, Nichol MC, Kuhse J, Betz H, Sanes JR (1998) Dual requirement for gephyrin in glycine receptor clustering and molybdoenzyme activity. *Science* **282:** 1321–1324

Fischer F, Kneussel M, Tintrup H, Haverkamp S, Rauen T, Betz H, Wassle H (2000) Reduced synaptic clustering of GABA and glycine receptors in the retina of the gephyrin null mutant mouse. *J Comp Neurol* **427:** 634–648

Freund TF (2003) Interneuron diversity series: rhythm and mood in perisomatic inhibition. *Trends Neurosci* **26:** 489–495

Fuhrmann JC, Kins S, Rostaing P, El Far O, Kirsch J, Sheng M, Triller A, Betz H, Kneussel M (2002) Gephyrin interacts with dynein light chains 1 and 2, components of motor protein complexes. *J Neurosci* **22:** 5393–5402

Geiger JR, Bischofberger J, Vida I, Frobe U, Pfitzinger S, Weber HJ, Haverkampf K, Jonas P (2002) Patch-clamp recording in brain slices with improved slicer technology. *Pflugers Arch* **443:** 491–501

Gerlai R, Henderson JT, Roder JC, Jia Z (1998) Multiple behavioral anomalies in GluR2 mutant mice exhibiting enhanced LTP. *Behav Brain Res* **95:** 37–45

Giesemann T, Schwarz G, Nawrotzki R, Berhorster K, Rothkegel M, Schluter K, Schrader N, Schindelin H, Mendel RR, Kirsch J, Jockusch BM (2003) Complex formation between the postsynaptic scaffolding protein gephyrin, profilin, and mena: a possible link of the microfilament system. *J Neurosci* **23:** 8330–8339

Gomeza J, Ohno K, Hulsmann S, Armsen W, Eulenburg V, Richter DW, Laube B, Betz H (2003) Deletion of the mouse glycine transporter 2 results in a hyperekplexia phenotype and postnatal lethality. *Neuron* **40:** 797–806

Grosskreutz Y, Hermann A, Kins S, Fuhrmann JC, Betz H, Kneussel M (2001) Identification of a gephyrin-binding motif in the GDP/GTP exchange factor collybistin. *Biol Chem* **382:** 1455–1462

Harvey K, Duguid IC, Alldred MJ, Beatty SE, Ward H, Keep NH, Lingenfelter SE, Pearce BR, Lundgren J, Owen MJ, Smart TG, Lüscher B, Rees MI, Harvey RJ (2004a) The GDP−GTP exchange factor collybistin: an essential determinant of neuronal gephyrin clustering. *J Neurosci* **24:** 5816–5826

Harvey RJ, Depner UB, Wassle H, Ahmadi S, Heindl C, Reinold H, Smart TG, Harvey K, Schutz B, Abo-Salem OM, Zimmer A, Poisbeau P, Welzl H, Wolfer DP, Betz H, Zeilhofer HU, Muller U (2004b) GlyR alpha3: an essential target for spinal PGE2-mediated inflammatory pain sensitization. *Science* **304:** 884–887

Huh GS, Boulanger LM, Du H, Riquelme PA, Brotz TM, Shatz CJ (2000) Functional requirement for class I MHC in CNS development and plasticity. *Science* **290:** 2155–2159

Kins S, Betz H, Kirsch J (2000) Collybistin, a newly identified brain-specific GEF, induces submembrane clustering of gephyrin. *Nat Neurosci* **3:** 22–29

Kirsch J, Betz H (1995) The postsynaptic localization of the glycine receptor-associated protein gephyrin is regulated by the cytoskeleton. *J Neurosci* **15:** 4148–4156

Kirsch J, Wolters I, Triller A, Betz H (1993) Gephyrin antisense oligonucleotides prevent glycine receptor clustering in spinal neurons. *Nature* **366:** 745–748

Kneussel M, Betz H (2000) Clustering of inhibitory neurotransmitter receptors at developing postsynaptic sites: the membrane activation model. *Trends Neurosci* **23:** 429–435

Kneussel M, Brandstatter JH, Gasnier B, Feng G, Sanes JR, Betz H (2001a) Gephyrin-independent clustering of postsynaptic $GABA_A$ receptor subtypes. *Mol Cell Neurosci* **17:** 973–982

Kneussel M, Brandstatter JH, Laube B, Stahl S, Muller U, Betz H (1999) Loss of postsynaptic $GABA_A$ receptor clustering in gephyrin-deficient mice. *J Neurosci* **19:** 9289–9297

Kneussel M, Engelkamp D, Betz H (2001b) Distribution of transcripts for the brain-specific GDP/GTP exchange factor collybistin in the developing mouse brain. *Eur J Neurosci* **13:** 487–492

Knuesel I, Mastrocola M, Zuellig RA, Bornhauser B, Schaub MC, Fritschy JM (1999) Short communication: altered synaptic

clustering of $GABA_A$ receptors in mice lacking dystrophin (mdx mice). *Eur J Neurosci* **11:** 4457–4462

Kuhn R, Schwenk F, Aguet M, Rajewsky K (1995) Inducible gene targeting in mice. *Science* **269:** 1427–1429

Levi S, Logan SM, Tovar KR, Craig AM (2004) Gephyrin is critical for glycine receptor clustering but not for the formation of functional GABAergic synapses in hippocampal neurons. *J Neurosci* **24:** 207–217

Lüscher B, Keller CA (2004) Regulation of GABAA receptor trafficking, channel activity, and functional plasticity of inhibitory synapses. *Pharm Therap* **102:** 195–221

Maas C, Tagnaouti N, Loebrich S, Behrend B, Lappe-Siefke C, Kneussel M (2006) Neuronal cotransport of glycine receptor and the scaffold protein gephyrin. *J Cell Biol* **172:** 441–451

Mammoto A, Sasaki T, Asakura T, Hotta I, Imamura H, Takahashi K, Matsuura Y, Shirao T, Takai Y (1998) Interactions of drebrin and gephyrin with profilin. *Biochem Biophys Res Commun* **243:** 86–89

Meyer G, Kirsch J, Betz H, Langosch D (1995) Identification of a gephyrin binding motif on the glycine receptor beta subunit. *Neuron* **15:** 563–572

Migaud M, Charlesworth P, Dempster M, Webster LC, Watabe AM, Makhinson M, He Y, Ramsay MF, Morris RG, Morrison JH, O'Dell TJ, Grant SG (1998) Enhanced long-term potentiation and impaired learning in mice with mutant postsynaptic density-95 protein. *Nature* **396:** 433–439

Moss SJ, Smart TG (2001) Constructing inhibitory synapses. *Nat Rev Neurosci* **2:** 240–250

Paarmann I, Schmitt B, Meyer B, Karas M, Betz H (2006) Mass spectrometric analysis of glycine receptor-associated gephyrin splice variants. *J Biol Chem* **281:** 34918–34925

Prior P, Schmitt B, Grenningloh G, Pribilla I, Multhaup G, Beyreuther K, Maulet Y, Werner P, Langosch D, Kirsch J, Betz H (1992) Primary structure and alternative splice variants of gephyrin, a putative glycine receptor-tubulin linker protein. *Neuron* **8:** 1161–1170

Ramming M, Kins S, Werner N, Hermann A, Betz H, Kirsch J (2000) Diversity and phylogeny of gephyrin: tissue-specific splice variants, gene structure, and sequence similarities to molybdenum cofactor-synthesizing and cytoskeleton-associated proteins. *Proc Natl Acad Sci USA* **97:** 10266–10271

Reid T, Bathoorn A, Ahmadian MR, Collard JG (1999) Identification and characterization of hPEM-2, a guanine nucleotide exchange factor specific for Cdc42. *J Biol Chem* **274:** 33587–33593

Rosch H, Schweigreiter R, Bonhoeffer T, Barde YA, Korte M (2005) The neurotrophin receptor p75NTR modulates long-term depression and regulates the expression of AMPA receptor subunits in the hippocampus. *Proc Natl Acad Sci USA* **102:** 7362–7367

Sassoe-Pognetto M, Panzanelli P, Sieghart W, Fritschy JM (2000) Colocalization of multiple $GABA_A$ receptor subtypes with gephyrin at postsynaptic sites. *J Comp Neurol* **420:** 481–498

Schmidt A, Hall A (2002) Guanine nucleotide exchange factors for Rho GTPases: turning on the switch. *Genes Dev* **16:** 1587–1609

Sola M, Bavro VN, Timmins J, Franz T, Ricard-Blum S, Schoehn G, Ruigrok RWH, Paarmann I, Saiyed T, O'Sullivan GA, Schmitt B, Betz H, Weissenhorn W (2004) Structural basis of dynamic glycine receptor clustering by gephyrin. *EMBO J* **23:** 2510–2519

Thiesen S, Kubart S, Ropers HH, Nothwang HG (2000) Isolation of two novel human RhoGEFs, ARHGEF3 and ARHGEF4, in 3p13−21 and 2q22. *Biochem Biophys Res Commun* **273:** 364–369

Ule J, Jensen KB, Ruggiu M, Mele A, Ule A, Darnell RB (2003) CLIP identifies Nova-regulated RNA networks in the brain. *Science* **302:** 1212–1215

Vaillend C, Billard JM, Laroche S (2004) Impaired long-term spatial and recognition memory and enhanced CA1 hippocampal LTP in the dystrophin-deficient Dmd(mdx) mouse. *Neurobiol Dis* **17:** 10–20

Zeng H, Chattarji S, Barbarosie M, Rondi-Reig L, Philpot BD, Miyakawa T, Bear MF, Tonegawa S (2001) Forebrain-specific calcineurin knockout selectively impairs bidirectional synaptic plasticity and working/episodic-like memory. *Cell* **107:** 617–629